Test of response linearity for magnetic force microscopy data

R. Yongsunthon and E. D. Williams[a]
Department of Physics, University of Maryland, College Park, Maryland 20742

J. McCoy and R. Pego
Department of Mathematics, University of Maryland, College Park, Maryland 20742

A. Stanishevsky
Laboratory for Ion Beam Research and Applications, University of Maryland, College Park, Maryland 20742

P. J. Rous
Department of Physics, University of Maryland, Baltimore County, Maryland 21250

The utility of vertical propagation by the Green's function to test response linearity has been explored for magnetic force microscopy (MFM) data from current-carrying wires, by comparing the measured signal at various tip heights to the corresponding propagated MFM signals. Application of a one-dimensional Green's function was found to be sufficient to predict signal height variation for sample regions of high to moderate field symmetry. For regions of high field asymmetry, the two-dimensional Green's function was required to obtain good prediction of the height variation. Agreement between the measured and propagated signals was generally within 5%, except at the tails where the signal is not well behaved. The quality of agreement deteriorates gradually with the size of the height propagation. The good agreement spanning a decade of tip and sample separation suggests that the MFM signal is not significantly affected by nonlinearities and can thus be interpreted in terms of classical electromagnetic relations governing current flow. © *2002 American Institute of Physics.* [DOI: 10.1063/1.1489701]

INTRODUCTION

Variations in current density near defects, constrictions, and corners in current-carrying lines may play a role in electromigration-induced failure.[1–3] Various groups have previously used magnetic force microscopy (MFM) to image current-carrying lines, in applications including detection of conducting paths for the purpose of IC failure analysis,[4] measurements of tip magnetization,[5,6] and instrumental development.[7] We have undertaken quantitative MFM imagery of current-carrying lines for the purpose of determining the underlying current density and variations in such. We have recently shown that MFM has sufficient sensitivity to detect variations in the magnetic field near micron-scale defects in current-carrying lines.[8] Semiquantitative analysis of the signal variation showed that the observed variations were consistent with the formation of a nonuniform current density near the defect. A full analysis of MFM signals to extract detailed information about the spatial distribution of the current density would be highly desirable. A necessary prerequisite for such an analysis is that the measured signal be cleanly interpretable, e.g., without serious perturbation due to interfering signals, instrumental effects, or changes in tip magnetization, in terms of the classical electromagnetic relationships governing current flow. To demonstrate that this is indeed the case, we here test the variation of MFM signal with tip height against the height variation predicted using Green's function propagation. If the MFM response is linear, consistency between the signals at various heights and the

signals propagated (from a lower height) must occur where there is no rotation in magnetic field. This is a necessary condition that must be satisfied for rigorous, quantitative interpretation of MFM data. Consistency of MFM data with the Green's function also ensures that the standard techniques for deconvolution in Fourier space[9–11] are valid. We have previously shown[12] that Green's function propagation can be used to construct a useful deconvolution approach for extremely narrow features. Here, we concentrate on the propagation properties of the measured signal, i.e., the true signal as convolved with the instrument response and affected by noise and interfering signals. Schendel *et al.*[11] have previously done similar analysis in Fourier space for magnetic thin films, but their analysis was limited to one relatively small (22 nm) height variation. Here, we perform a study that spans a decade of tip and sample separation, with linear lift heights ranging from 200 to 1600 nm (corresponding tip and sample separations from 90 to 1490 nm), and use a current-carrying line with clear fiducials that allow us to precisely locate the points of comparison.

The measured MFM signal, $D(x,y,z)$, obtained at tip height z is a three-dimensional instrumental convolution,

$$
\begin{aligned}
D(x,y,z) &= \int\int\int A(x-x',y-y',z-z') \\
&\quad \times f(x',y',z')dx'dy'dz' \\
&= \int\int\int A(x',y',z')f(x-x',y-y',z-z') \\
&\quad \times dx'dy'dz',
\end{aligned}
\tag{1}
$$

[a]Electronic mail: edw@physics.umd.edu

over the instrumental response function $A(x,y,z)$ and the unknown true signal $f(x,y,z)$. Standard MFM is operated in phase detection mode, where the signal measured is a phase shift. If the tip is modeled as a point dipole (with magnetic moment m_z), the phase shift relates to the field curvature as

$$d\varphi = -\left(\frac{Q}{k}\right)m_z\frac{\partial^2 B_z}{\partial z^2}, \qquad (2)$$

where Q and k are parameters of the specific instrument and B_z is the vertical component of the magnetic field (perpendicular to the sample). We use the extended charge model of the tip, accounting for the observed signal broadening by convolution of Eq. (2) with an instrumental response function.[12,13] Other groups have found that the monopole model is often a better empirical model of the tip if it is approximated as a point probe.[11,14–16] As previously discussed for the case of a current-carrying wire aligned parallel to the y axis,[12] since $\nabla\times\mathbf{H}$ vanishes above the sample,

$f(x,y,z+\Delta z)$, which is proportional to the curvature of the magnetic field, can be written as a convolution over $f(x,y,z)$. When geometric symmetry permits neglecting variation along the y direction, we have

$$f(x,y,z+\Delta z) = \int G(x-\bar{x},\Delta z)f(\bar{x},y,z)d\bar{x}$$

$$= \int G(\bar{x},\Delta z)f(x-\bar{x},y,z)d\bar{x}, \qquad (3)$$

where the one-dimensional (1D) Green's function has the form

$$G(x,z) = \frac{z}{\pi}\frac{1}{x^2+z^2}. \qquad (4)$$

The Green's function propagation also holds for the measured signal [Eq. (1)]. We can show this, using commutation properties:

$$\int G(x-\bar{x},\Delta z)D(\bar{x},y,z)d\bar{x} = \int G(\bar{x},\Delta z)D(x-\bar{x},y,z)d\bar{x}$$

$$= \int G(\bar{x},\Delta z)\int\int\int A(x',y',z')f(x-\bar{x}-x',y-y',z-z')dx'dy'dz'd\bar{x}$$

$$= \int\int\int A(x',y',z')\int G(\bar{x},\Delta z)f(x-x'-\bar{x},y-y',z-z')d\bar{x}dx'dy'dz'$$

$$= \int\int\int A(x',y',z')f(x-x',y-y',z+\Delta z-z')dx'dy'dz' = D(x,y,z+\Delta z). \qquad (5)$$

This result can be generalized to cases where there is no y-axis symmetry, e.g., a wire containing defects, using two-dimensional (2D) propagation

$$D(x,y,z+\Delta z) = \int\int G(x-\bar{x},y-\bar{y},\Delta z)D(\bar{x},\bar{y},z)d\bar{x}d\bar{y}, \qquad (6)$$

where the 2D Green's function has the form

$$G(x,y,z) = \frac{z}{2\pi}\left(\frac{1}{x^2+y^2+z^2}\right)^{3/2}. \qquad (7)$$

Equations (5) and (6) are based purely on classical electromagnetic relations and provide a relationship that can be directly used to test the assumptions we make regarding MFM response.

EXPERIMENTAL TECHNIQUE

Experiments were performed using a Digital Instruments Multimode, operated in tapping (intermittent contact) and standard MFM phase detection modes. The signal detected is proportional to the curvature of the magnetic field component perpendicular to the sample plane [Eq. (2)]. The magnetic tips used are commercially available Co/Cr coated Digital Instruments MESP-HM tips, magnetized along the

tip axis, perpendicular to the sample surface. Calibration of the piezoelectric scanners was performed using Digital Instruments standards and methods. Vertical displacement linearity is expected to be ±3% for heights on the order of 300 nm, but the calibration may not hold in the micron range.

The sample used for this study was fabricated using a combination of standard photolithography/lift-off and focused ion beam (FIB) milling techniques. A blank metal line was created on thermally grown SiO_2 by photolithography, followed by thermal evaporation of 20 nm Cr and 110 nm Au, and liftoff. A 1×9 μm slit, slanted at 45° relative to the metal line, was fabricated in a 12-μm-wide metal line by FIB milling.[17] Ion milling was performed with 50 kV Ga^+ ions using a Micrion 2500 FIB machine with a 5 nm beam column. A serpentine beam scanning procedure and relatively low ion current (~30 pA) were chosen to provide a better slit shape.

MFM measurements were made with typical currents in the individual lines of about 33 mA, corresponding to current densities on the order of $2-8\times10^6$ A/cm^2. To exclude topographical artifacts, the MFM phase measurements were performed in Digital Instruments interleave linear lift mode,[18,19] using lift heights ranging from 200 to 1600 nm. In linear lift mode, the tip is lifted along a linear path at a constant height offset above a specific linear base line, which is dependent

upon the topography. (This mode is different from the standard lift mode generally used, where the tip is lifted by a height offset above the measured surface topography. For our sample topography and specific scan size, the corresponding standard lift height is 110 nm lower than our linear lift height in regions above the metal line, i.e., 200 nm linear lift corresponds to a standard lift of 90 nm, 400 nm linear lift corresponds to 290 nm, etc.) For current-carrying lines, where there are abrupt and often large ($>$100 nm) changes in height near the conductor sidewalls, linear lift mode ensures that the same active volume of the tip interacts with the sample as the tip is scanned across the linewidth. This is essential to avoid topography artifacts in these measurements. To exclude phase response due to electrostatic forces, the potential between the tip and sample was nulled by an external voltage divider, as discussed in previous work.[19,20]

In spite of the measures taken to eliminate nonmagnetic contributions to the phase signal, the measurements often have asymmetric backgrounds that cannot be physically eliminated. These backgrounds can result from unquantified long-range interactions of the conducting magnetic tip/cantilever and other parts of the sample, such as the large contact pads. Typical backgrounds minimally affect the signal's high-magnitude regions of interest but can greatly affect the behavior of the data tails. When significant, these backgrounds are subtracted from the data, e.g., such that a reference signal has the required symmetry and characteristics.

In addition to the physical aspects of the experiment, the practical issues of analysis must be also considered. Due to scanning limitations (512 data points per line scan and a maximum scan range of about 120 μm), we take relatively small scans to optimize the image resolution. The small scan range can affect the numerical implementation of the convolution of Eqs. (5) and (6). If the data scan is truncated before the signal adequately decays, the effectively smaller integration areas near the ends of the scan will result in error at the ends of the convolution. Where possible, we choose scan sizes that compromise between optimal image resolution and well-behaved tails in the scan.

Interpretation of the data assumes the permanence of the tip magnetization and that the effective magnetization is unaffected by the tip position relative to the sample. Another assumption is the linearity of Eq. (2), which is based upon the first-order expansion of the phase, with respect to perturbation in effective cantilever stiffness near resonance, which relates a shift in phase to the force gradient. Calculations of the expected force gradients, given approximate tip magnetization and current densities, indicate that the first-order expansion is sufficient for our low phase shifts. Similarly, a related concern is the linearity of the instrumental output. The Digital Instruments NanoScopeIIIa extender box actually outputs $\cos(90° + \text{phase shift})$, rather than the true phase shift as measured with a lock-in technique (by "phase," we typically mean the change in phase from 90° at resonance). Since our maximum phase shift magnitude is on the order of 3°, we typically assume that the approximate phase obtained is accurate for our purposes. Significant failure of any of
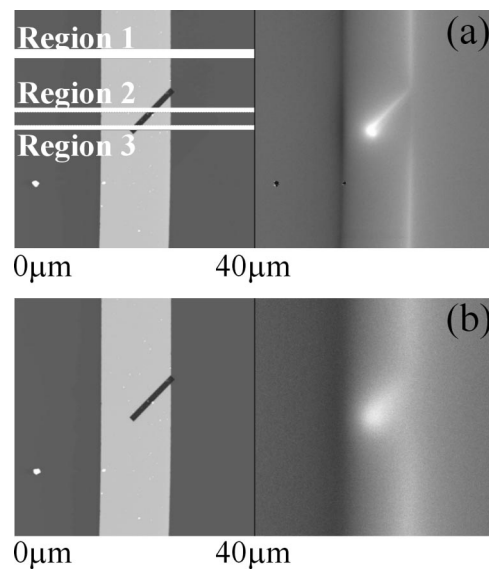

FIG. 1. 40$\times$40 μm image of a 12 μm line with a 1$\times$9 μm 45°-slanted slit on one side. This line is carrying a 33 mA current, corresponding to a 2.5 $\times 10^6$ A/cm^2 current density. Left: AFM topography (z range: 300 nm). The MFM line scans from region 1 were averaged to obtain a reference line scan; MFM line scans from region 2 were averaged to obtain a line scan along the slit midpoint; and MFM line scans from region 3 were averaged to obtained a line scan along the slit edge.   (a) Left: AFM topography (z range: 300 nm). Right: corresponding MFM phase measured with 200 nm linear lift height (z range: 4.0°).   (b) Left: AFM topography (z range: 300 nm). Right: corresponding MFM phase measured with 1600 nm linear lift height (z range: 2.0°).

these linearity assumptions would cause the measurements to deviate from the Green's function prediction.

EXPERIMENTAL RESULTS

A tapping atomic force microscopy (AFM) image of the sample with a fabricated slit and the corresponding MFM phase image at 200 nm linear lift height are shown in Fig. 1(a). Given the vertical tip magnetization, there is MFM contrast only at the line edges where the magnetic field must curve into or out of the sample plane. There is significantly higher contrast at the slit edge than at the line edge on the side opposite the slit. This is due to a localized increase in the current density (current crowding) near the slit edge.[8,13] The two dark spots in the lower half of the MFM image of Fig. 1(a) are due to the presence of the large dust particles in the topography and were removed for the analysis. A tapping AFM image of the slit and the corresponding MFM phase image at 1600 nm linear lift height are shown in Fig. 1(b). Although qualitatively similar to the 200 nm lift height image in Fig. 1(a), there is significant reduction in signal magnitude, sharpness, and contrast. Images were also taken at linear lift heights of 400 and 800 nm, and they show similar blurring to lesser degrees. The background in this data set was small, so no subtraction was performed on these measurements.

In order to test the responsiveness of MFM data to vertical propagation by the Green's function, we take line scans along the image captured at 200 nm lift height, propagate them to various heights, using Eqs. (5) and (6), and compare the results to the actual data from those heights. The least demanding test is for a line scan in the region far from the
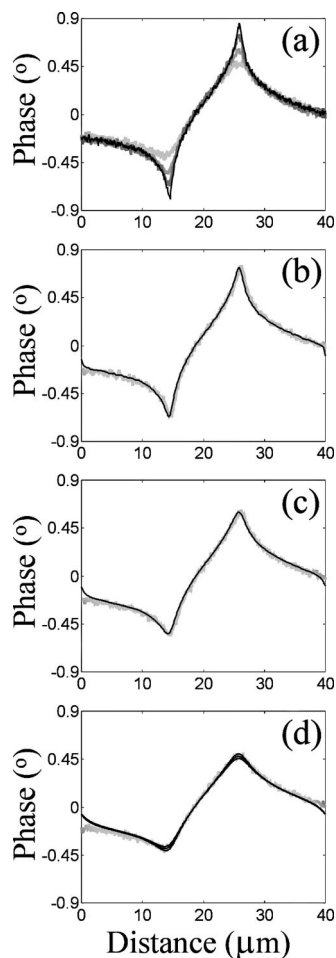
FIG. 2. Reference MFM line scan, averaged from the portion of the MFM image corresponding to region 1 of Fig. 1(a). (a) MFM line scans across the line, averaged over a 0.86 μm segment (11 of 512 line scans), 10 μm away from the slanted slit. In order of descending signal magnitude, the averaged line scans correspond to linear lift heights of 200, 400, 800, and 1600 nm. In (b)–(d) the bold gray line is the averaged line scan measured at linear lift height Z, and the thin dark line is the corresponding 1D Green's function propagation from the data taken at 200 nm linear lift height. (b) Z=400 nm; (c) Z=800 nm; and (d) the three thin dark lines correspond, in order of descending magnitude, to the propagations at 1440, 1600, and 1760 nm, and provide a measure of the effect of ±10% error on the actual piezo height.

slit, where the line has the greatest local symmetry and can be used as a defect-free reference. MFM line scans across the sample, averaged over a 0.86 μm segment (11 of 512 line scans) about 10 μm away from the slanted slit, are shown in Fig. 2(a). In order of descending signal magnitude, the averaged line scans correspond to linear lift heights of 200, 400, 800, and 1600 nm. The bold gray line of Fig. 2(b) is the averaged line scan at 400 nm linear lift height, and the thin dark line is the corresponding 1D Green's function propagation from the data taken at 200 nm linear lift height. The discrepancy between the actual data and the propagation is generally within 5%, except at the beginning and end of the line scans, where the effects of the data tails are important, as discussed earlier. The corresponding plots are shown in Figs. 2(c) and 2(d) for linear lift heights of 800 and 1600 nm, respectively. The agreement between the raw data and the propagated signal is again very good, with the discrepancy

increasing slightly with the size of the height propagation. Figure 2(d) includes three thin dark lines that correspond, in order of descending magnitude, to the propagations at 1440, 1600, and 1760 nm, and provide a measure of the effect of ±10% error on the actual piezo height. Of the three curves shown, the propagation to 1600 nm is most consistent with the actual data and it is unlikely that there is some unaccounted for effect that automatically corrects for inaccurate piezoresponse. Figure 2(d) thus suggests that our piezo height behavior is good to well within 10%, even at large lift heights.

A more demanding test of the Green's function propagation is for a line scan from the region along the midpoint of the slit, where the current is subjected to narrowing of the effective linewidth. MFM line scans across the sample, averaged over a 0.23 μm segment (3 of 512 line scans) along the lengthwise midpoint of the slit, are shown in Fig. 3(a). In order of descending signal magnitude, the averaged line scans correspond to linear lift heights of 200, 400, 800, and 1600 nm. The MFM scans are higher in magnitude and more asymmetrical than those of the reference scan, because the current is being constricted to a higher overall density and there is some crowding on the slit side. The bold gray line of Fig. 3(b) is the averaged line scan at 400 nm linear lift height, and the thin dark line is the corresponding 1D Green's function propagation from the data taken at 200 nm linear lift height. The discrepancy between the actual data and the propagation is generally within 5%. The corresponding plots, shown in Figs. 3(c) and 3(d) for linear lift heights of 800 and 1600 nm, respectively, also demonstrate good agreement. Figure 3(d) includes three thin dark lines that correspond, in order of descending magnitude, to the propagations at 1440, 1600, and 1760 nm and provide a measure of the effect of ±10% error on the actual piezo height. The consistency between the propagations and the actual data indicate that the 1D Green's function propagation is quite robust, working well even for regions that are not bilaterally symmetric.

The most demanding test is for a line scan at the edge of the slit, where there is an abrupt change in effective linewidth. MFM line scans across the sample, averaged over a 0.23 μm segment (3 of 512 line scans) along the slit edge, are shown in Fig. 4(a). In order of descending signal magnitude, the averaged line scans correspond to linear lift heights of 200, 400, 800, and 1600 nm. The MFM scans are higher in magnitude and very asymmetrical compared to those of the reference scan, because the current is being constricted to a higher overall density and there is strong crowding near the slit edge. The 1D Green's function propagation was inadequate for this case, with discrepancies in MFM peak magnitude as high as 40%. The high discrepancy indicates the need for 2D treatment of samples that exhibit a high degree of asymmetry. The bold gray line of Fig. 4(b) is the averaged line scan at 400 nm linear lift height, and the thin dark line is the corresponding 2D Green's function propagation from the data taken at 200 nm linear lift height. The discrepancy between the actual data and the 2D propagation is generally within 5%. The corresponding plots, shown in Figs. 4(c) and 4(d) for linear lift heights of 800 and 1600 nm, respectively,
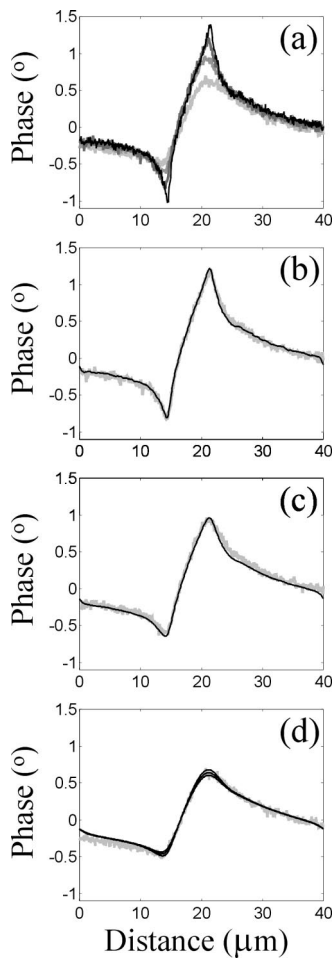
FIG. 3. MFM line scan along the slit midpoint, averaged from the portion of the MFM image corresponding to region 2 of Fig. 1(a). (a) MFM line scans across the line, averaged over a 0.23 μm segment (3 of 512 line scans) along the slit midpoint. In order of descending signal magnitude, the averaged line scans correspond to linear lift heights of 200, 400, 800, and 1600 nm. In (b)–(d) the bold gray line is the averaged line scan measured at linear lift height Z, and the thin dark line is the corresponding 1D Green's function propagation from the data taken at 200 nm linear lift height. (b) Z = 400 nm; (c) Z = 800 nm; and (d) the three thin dark lines correspond, in order of descending magnitude, to the propagations at 1440, 1600, and 1760 nm, and provide a measure of the effect of ±10% error on the actual piezo height.
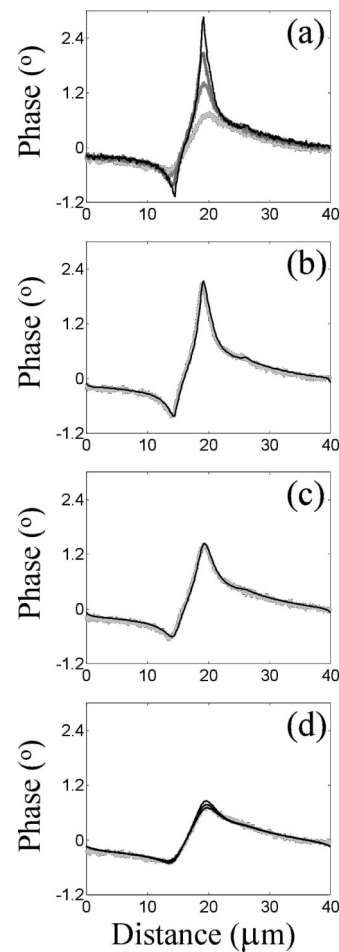
FIG. 4. MFM line scan along the slit edge, averaged from the portion of the MFM image corresponding to region 3 in Fig. 1(a). (a) MFM line scans across the line, averaged over a 0.23 μm segment (3 of 512 line scans) along the slit edge. In order of descending signal magnitude, the averaged line scans correspond to linear lift heights of 200, 400, 800, and 1600 nm. In (b)–(d) the bold gray line is the averaged line scan measured at linear lift height Z, and the thin dark line is the corresponding 2D Green's function propagation from the data taken at 200 nm linear lift height. (b) Z = 400 nm; (c) Z = 800 nm; and (d) the three thin dark lines correspond, in order of descending magnitude, to the propagations at 1440, 1600, and 1760 nm and provide a measure of the effect of ±10% error on the actual piezo height.

also demonstrate good agreement. Figure 4(d) includes three thin dark lines that correspond, in order of descending magnitude, to the propagations at 1440, 1600, and 1760 nm and provide a measure of the effect of ±10% error on the actual piezo height.

In all cases, the absolute MFM peak sizes are in excellent agreement, generally within 1%–3%. The signature of the current crowding phenomenon that we wish to observe is primarily contained in the MFM peaks. Although the tails are of lesser importance, they do affect the deconvolution of the data and must be treated on a case-by-case basis, e.g., by appropriate background subtraction. The interpretations of any analysis must always consider the lower reliability of results at the tails, where even small backgrounds may have a large effect.

CONCLUSION

Magnetic force microscopy data from current-carrying lines have been shown to be robust with regard to propagation of lift height by the Green's function. The agreement between the raw data and the propagated data was generally within 5%, except at tails where the signal is not well behaved. This result shows that the measured MFM signal is linear to within 5% and is consistent with the fundamental requirements of classical electromagnetic relationships. Assuming no cancellation between different sources of nonlinearity, the agreement also suggests that the tip magnetization is constant to within 5%, in the presence of the relatively weak fields of our current-carrying line. Thus, in-depth analysis of the MFM signals to extract quantitative information about the underlying current distributions is warranted. The 1D Green's function proved to be sufficient for treatment of data from regions of high to moderate symmetry,

such as those far from the slit or on the slit midpoint. For data from regions of extreme asymmetry, such as scans taken along the slit edge, using the full 2D Green's function propagation was necessary to obtain reasonable agreement. Although not a complete check of linearity (accidental cancellation of different sources of nonlinearity could occur), a test of the Green's function propagation can be used as a necessary prerequisite for rigorous physical analysis of any MFM data.

ACKNOWLEDGMENTS

[1] P. F. Tang, in *Electromigration and Electronic Device Degradation*, edited by A. Christou (1994), pp. 27–77.

[2] K. N. Tu, C. C. Yeh, C. Y. Liu, and C. Chen, Appl. Phys. Lett. **76**, 988 (2000).

[3] E. C. C. Yeh and K. N. Tu, J. Appl. Phys. **88**, 5680 (2000).

[4] A. N. Campbell, J. E. I. Cole, B. A. Dodd, and R. E. Anderson, Proceedings of the 31st Annual IEEE International Reliability Physics (1993), pp. 168–177.

[5] R. D. Gomez, A. O. Pak, A. J. Anderson, E. R. Burke, A. J. Leyendecker, and I. D. Mayergoyz, J. Appl. Phys. **83**, 6226 (1998).

[6] L. Kong and S. Y. Chou, Appl. Phys. Lett. **70**, 2043 (1997).

[7] T. Alvarez, S. V. Kalinin, and D. A. Bonnell, Appl. Phys. Lett. **78**, 1005 (2001).

[8] R. Yongsunthon, A. Stanishevsky, J. McCoy, and E. D. Williams, Appl. Phys. Lett. **78**, 2661 (2001).

[9] J.-G. Zhu, X. Lin, and S. Rick C, J. Appl. Phys. **83**, 6223 (1998).

[10] T. Chang, M. Lagerquist, J.-G. Zhu, J. H. Judy, P. B. Fischer, and S. Y. Chou, IEEE Trans. Magn. **28**, 3138 (1992).

[11] P. J. A. van Schendel, H. J. Hug, B. Stiefel, S. Martin, and H.-J. Guntherodt, J. Appl. Phys. **99**, 435 (2000).

[12] J. McCoy, R. Pego, R. Yongsunthon, A. Stanishevsky, and E. D. Williams (unpublished).

[13] P. J. Rous, R. Yongsunthon, J. McCoy, A. Stanishevsky, and E. D. Williams (unpublished).

[14] S. McVitie, R. P. Ferrier, J. Scott, G. S. White, and A. Gallagher, J. Appl. Phys. **89**, 3656 (2001).

[15] J. Lohau, S. Kirsch, A. Carl, G. Dumpich, and E. F. Wassermann, J. Appl. Phys. **86**, 3410 (1999).

[16] G. D. Skidmore and E. D. Dahlberg, Appl. Phys. Lett. **71**, 3293 (1993).

[17] J. Melngailis, J. Vac. Sci. Technol. B **5**, 469 (1987).

[18] Digital Instruments technical support (private communication).

[19] R. Yongsunthon, J. McCoy, and E. D. Williams, Proceedings of the ULSI Metrology Conference (2000), Vol. 550, pp. 630–634.

[20] R. Yongsunthon, J. McCoy, and E. D. Williams, J. Vac. Sci. Technol. **19**, 1763 (2001).